JOURNAL OF OPTOELECTRONICS AND ADVANCED MATERIALS Vol. 15, No. 7- 8, September – October 2013, p. 948 - 953

Germanium solar cells prepared by ion implantation

ISMAIL KABACELIK[*], RASIT TURAN[a,b,c]

[*] *Department of Physics, Faculty of Sciences, Akdeniz University, Campus 07058, Antalya, Turkey*

[a] *Department of Physics, Middle East Technical University, Dumlupınar Bulvarı, No : 1, 06800, Ankara, Turkey*

[b] *The Center for Solar Energy Research and Applications (GÜNAM), Middle East Technical University, Dumlupınar Bulvarı, No: 1, 06800, Ankara, Turkey*

[c] *Micro and Nanotechnology Graduate Program, Middle East Technical University, Dumlupınar Bulvarı, No : 1, 06800, Ankara, Turkey*

Development of Ge solar cells for multijunction solar cells, where the p-n junction is formed by ion implantation is investigated. Ge samples are doped by phosphorus (P) ions having 60 keV energy at dose ratios of $1x10^{13}$, $1x10^{14}$, $1x10^{15}$ ve $1x10^{16}$ ions/cm^2 at room temperature. The influences of P concentration and activation temperature on Ge solar cells is investigated. P concentration and layer resistance are measured by secondary ion mass spectrometry (SIMS) and a 4-point probe, respectively. Layer resistances of Ge samples are observed to vary as a function of concentration and temperature. The short circuit currents (I_{sc}) and open circuit voltages (V_{oc}) of the Ge solar cells is compared through examination of the I-V curves of the cells with respect to concentration and temperature. Besides, α-Si thin films are introduced as anti-reflection coatings (ARCs) via DC sputtering method and the impact of ARCs on I_{sc} and V_{oc} is investigated. The ARCs is observed to increase the I_{sc}'s of all four samples with respect to uncoated samples.

(Received July 29, 2013; accepted September 18, 2013)

Keywords: Germanium, Ion-implantation, Solar cell

---

1. Introduction

In recent years, the fact that Germanium (Ge) is used in many application domains such as CMOS [1,2], photodetectors [2,3] and solar cells [4,5], has been a focus of interest amongst the scientist working in this field. Large electron and hole mobilities in Ge and relatively large absorption coefficient make Ge a good candidate for CMOS and photodetectors based on Ge. Since Ge has a band gap of 0,67 eV at room temperature (RT) (300 K), thus being able to absorb photons with wavelengths up to 1800 nm, it is especially important in high-efficiency solar cells and thermophotovoltaic (TPV) cells applications.

Lately, Ge-based solar cells are extensively studied due to the fact that Ge is lattice-matched to GaAs and that it is high mechanically strength than GaAs [6-15]. High-quality epitaxial growth of GaAs on Ge is carried out by MOCVD. Currently MOCVD is the standard technique for epitaxial growth of multi-junction solar cells such as AlGaAs/GaAs/Ge and GaInP/GaAs/Ge [16]. Ge p-n junction is formed by diffusion doping of Group III or V elements into Ge substrate [6]. Besides, it is proposed that Ge solar cells used as substrates in high-efficiency multi-junction solar cells [6-15] can also be utilized in Si/Ge tandem solar cells [17]. Along with diffusion of Group III or V elements, the p-n junction can also be formed by ion implantation [18]. Due to the ability to tightly control doping concentration and depth profile, ion implantation is a widely-used doping technique in semiconductor technology [19]. In this method, damage occurs in the implanted region due to interactions between the energetic ion species and the target material atoms. These damages lead to existence of localized electronic states within the band gap of the semiconductor and degrade device performance. By high-temperature annealing, the implanted ions move to electrically-active sites of the crystal lattice. The important parameters in ion implantation are implantation dose, energy, annealing temperature, period and atmosphere [20].

This work aims preparation of Ge solar cells used as substrates for III-V multi-junction solar cells and Si/Ge tandem solar cells by forming the p-n junction through ion implantation. Ge was doped with different P concentrations in order to achieve maximum efficiency for solar cells. The influences of P concentration and activation temperature on the current-voltage (I-V) curves of the solar cells are investigated and the open-circuit voltages (V_{oc}) and the short-circuit currents (I_{sc}) are compared. Besides, the influence of an anti-reflection coating (ARC) layer on the I-V curves of the solar cells is also investigated.

2. Experiment

The scope of the work is to develop the Ge substrate and p-n junction utilized as a basis for multi-junction solar cells. P-type Ge wafers (100) with 1-30 Ω.cm resistivity are used. The p-n junction within Ge is formed by ion implantation. No special surface preparation or cleaning was done prior to implantation. Ge samples are prepared at RT by 60 keV phosphorus (P) at dose ratios of $1x10^{13}$, $1x10^{14}$, $1x10^{15}$ and $1x10^{16}$ ions/cm^2. The ion beam is tilted

7° with respect to substrate surface normal to minimize channeling effects.

During P activation the Ge surface is cleaned first in a 10% HF solution for a period of 10 s. The chemical concentration of P ions is determined by TOF-SIMS analyses prior to annealing. In order to prevent escape of the P atoms implanted into Ge by ion implantation during annealing, the sample is coated by a 125 nm Si_3N_4 layer by magnetic sputtering. Si_3N_4 sputtering onto the P-implanted Ge samples is carried out by forming an Ar plasma. To make the P ions electrically-active, the Ge samples are annealed by Rapid Thermal Annealing (RTA) in Ar environment at 650 ^{o}C for 60 and 120 s. Moreover, annealing in a quartz tube furnace under N_2 environment at 700 ^{o}C for 30 minutes is applied. The Si_3N_4 layer over the surface is removed by 5% HF solution before the sheet resistance (Rs) measurements after annealing. The sheet resistances are measured at 5 different sites of the Ge samples by a 4-point probe.

A simple solar cell is formed by introducing back and front contacts into the P-implanted Ge samples by thermal evaporation for electrical measurements. First, the Al layer is deposited on the back face followed by 30-minute annealing at 420 ^{o}C and then the Ag layer is deposited on the front face to be annealed at 250 ^{o}C for 30 minutes. The I-V measurements are carried out under 0.1 W.cm^{-2} illumination. Furthermore, the ARC layers of 80 nm thickness are formed on the Ge samples by coating an amorphous Silicon (α-Si) thin film through DC sputtering and the influences of the ARC layers on the IV curves are investigated.

3. Results and discussion

The relative chemical concentration of P ions in Ge samples implanted by 60 keV P ions at RT at 1x10^{13}, 1x10^{14}, 1x10^{15} and 1x10^{16} ions/cm^{2} dose ratios are determined by Time-of-Flight Secondary Ion Mass Spectrometry (TOF-SIMS). The variations in the P concentration obtained at 4 different doses are presented in Fig. 1. No annealing is applied on the Ge samples prior to TOF-SIMS analyses. The depth profiles of the grooves appeared during the TOF-SIMS analyses are determined by profilometer and presented on Table 1.

After coating P-implanted Ge samples by Si_3N_4 through magnetic sputtering to prevent escape of the P ions, the samples are annealed at 650^{o}C for 60 and 120 s through RTA to achieve activation of P ions. Meanwhile, another sample set is annealed in a quartz tube furnace under N_2 environment at 700^{o}C for 30 minutes. Results of sheet R_s after removal of the Si_3N_4 layers by HF through 4-point probe measurements are presented on Table 2. The R_s values on Table 2 are the averages of the values measured at 5 different positions.

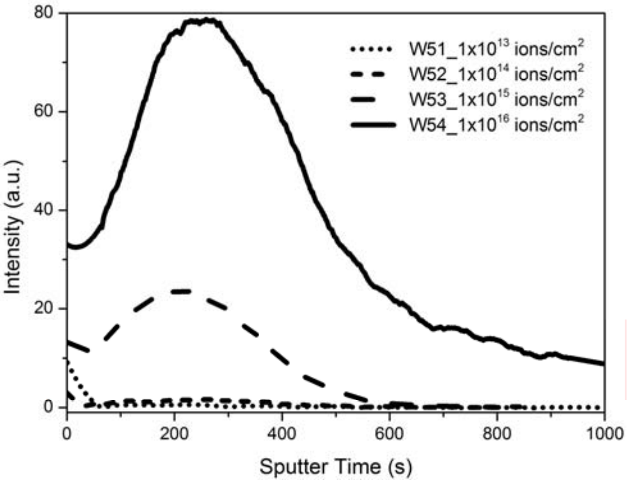

Fig. 1. The variations of relative $^{31}P^{+}$ concentrations for different implantation doses determined by TOF-SIMS.

Table 1: Depth profiles determined through profilometer.

Sample name	Dose (ions/cm^{2})	Depth (nm)
W51	1x10^{13}	85
W52	1x10^{14}	108
W53	1x10^{15}	177
W54	1x10^{16}	220

The R_s values of all samples, except W54 annealed through RTA at 650 ^{o}C for 60 and 120 s, tend to decrease with increasing concentration. There exist large fluctuations in the R_s values of the W54 sample, while the average of the 5 values is still larger than any R_s values measured on samples W51, W52 and W53. Cracks formed on the surface of W54 sample after RTA process. The SEM images and profilometer analyses of these cracks are presented in Fig. 2. The cracks observed after heat treatment are thought to appear due to over-dose in doping. The R_s values measured after 30-minute annealing in quartz tube furnace at 700 ^{o}C tend to decrease with increasing concentration. Contrary to the annealing by RTA, the R_s value of W54 sample is significantly smaller than that of the samples prepared at lower concentrations. Furthermore, the cracks observed in RTA process are not observed after annealing in quartz tube.

Table 2: The average sheet resistances after heat treatment of Ge samples prepared at four different doses.

	W51 (Ω/□) ($1x10^{13}$ ions/cm^2)	W52 (Ω/□) ($1x10^{14}$ ions/cm^2)	W53 (Ω/□) ($1x10^{15}$ ions/cm^2)	W54 (Ω/□) ($1x10^{16}$ ions/cm^2)
650 ^{o}C – 60 s (RTA)	250	165	48	305
650 ^{o}C – 120 s (RTA)	230	150	46	425
700 ^{o}C – 30 min (FA)	300	193	90	9

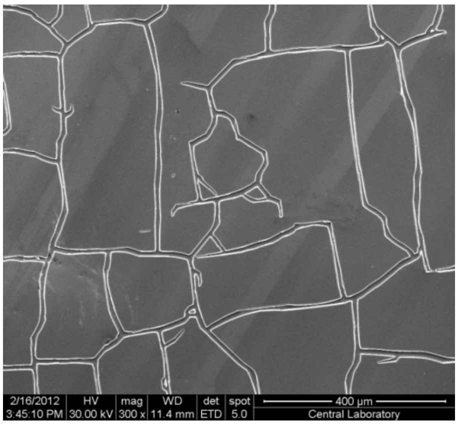

a

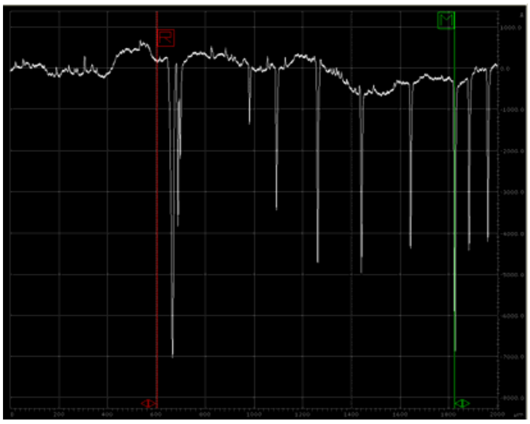

b

Fig. 2: The SEM image of the cracks appeared on the surface of W54 sample after heat treatment (a) and the depth profile analysis of these cracks (b). The profilometer data represents the fluctuations in the depth profile of the surface due to cracks.

The solar cell geometry shown in Fig. 3 depict the back and front contacts for electrical measurements formed by thermal evaporation over the Ge samples annealed under Ar environment at 650 ^{o}C for 60 and 120 s through RTA or annealed in a quartz tube under N_2 environment at 700 ^{o}C for 30 minutes. To reduce the photon numbers reflected off the surface, the surface of the samples are coated by 80 nm-thick α-Si ARC layers by DC sputtering and the influences of ARCs on the I-V curves are also investigated.

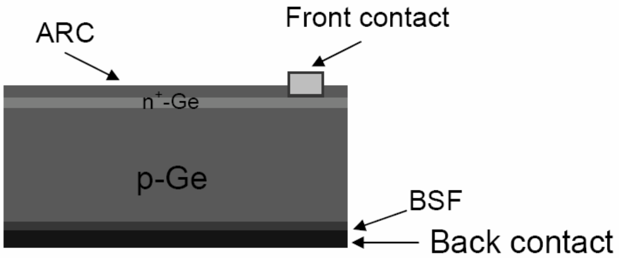

Fig. 3. The cross-section of the Ge solar cell produced.

Fig. 4 presents the I-V measurement results with or without ARCs of the samples W51, W52, W53 and W54 annealed at 650 ^{o}C for 60 s through RTA. The V_{oc} and I_{sc} values vary depending on P concentration. Both V_{oc} and I_{sc} of W51, W52 and W53 samples increase with concentration regardless of the existence of ARC layer. On the contrary, due the cracks formed during heat treatment of W54 sample, this sample does not exhibit the same trend.

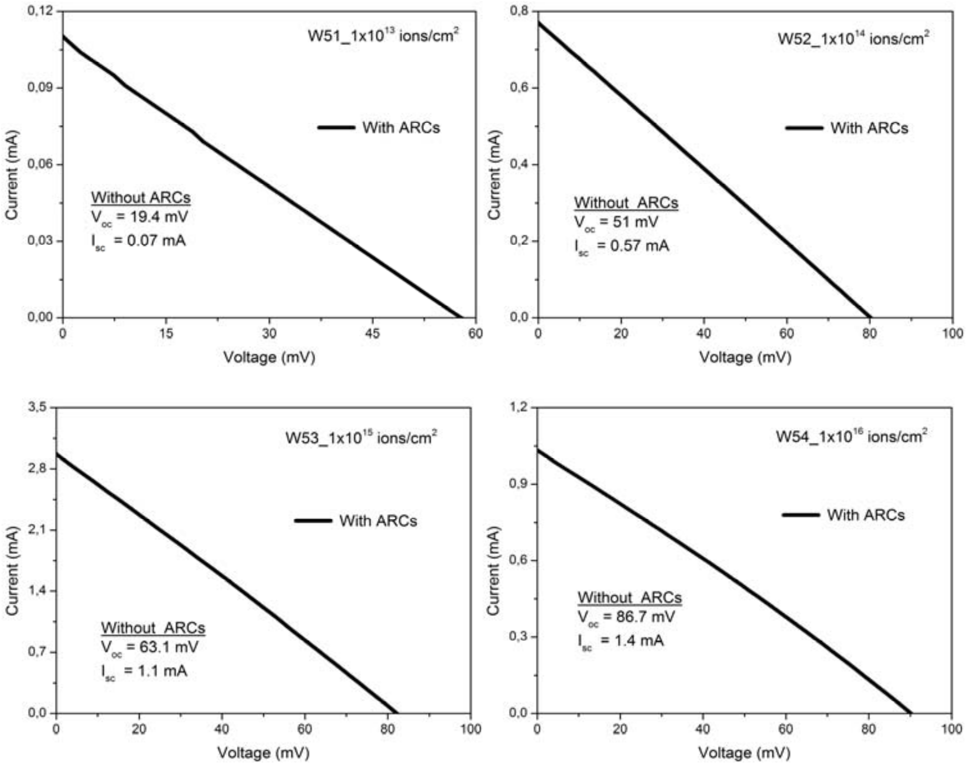

Fig. 4: The I-V measurement results of Ge samples implanted at different P concentrations after annealing at 650 °C for 60 s.

The I-V measurement results of W51, W52, W53 and W54 samples annealed at 650 °C for 120 s are presented in Fig. 5. The V_{oc} and I_{sc} of these samples also increase with increasing P concentration without regard to whether the samples are ARC coated. The I_{sc} values of W51, W52 and W53 samples are similar to those of the same samples annealed at 650 °C for 60 s. In contrast, the V_{oc} values are somewhat larger than those of the samples annealed at 650 °C for 60 s. The W54 sample, again, does not exhibit similar behavior with the other samples

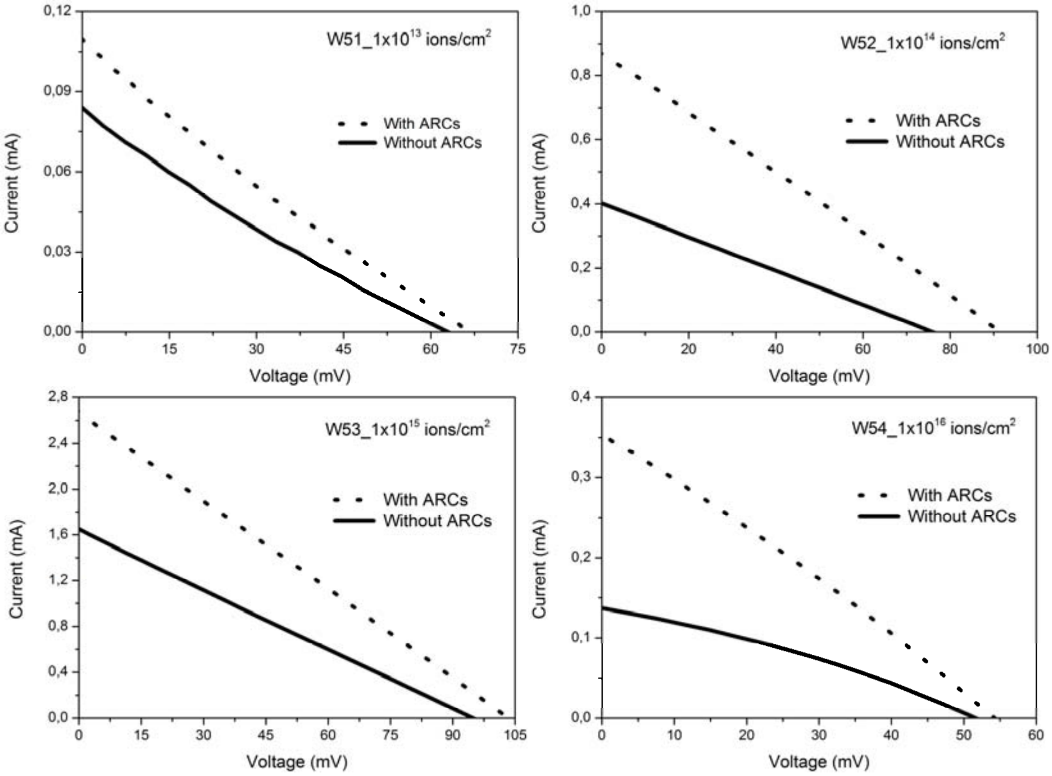

Fig. 5: The I-V measurement results of Ge samples implanted at different P concentrations after annealing at 650 °C for 120 s.

The I_{sc} and V_{oc} values of the samples annealed at 650 °C for 60 s and 650 °C for 120 s in RTA under Ar flow are given in Table 3 for comparison from the I-V curves at Fig. 4 and Fig. 5. From Table 3, it can be seen that the Isc and Voc values of sample W53 with $1x10^{15}$ ions/cm^2 doping has the highest values. In order to obtain maximum V_{oc} and I_{sc} from this sample, the effect of annealing temperature and duration on I_{sc} and V_{oc} can be investigated.

Besides heat treatment by RTA, another sample set is annealed in a quartz tube furnace under N_2 environment at 700 °C for 30 minutes. The I-V measurement results of these samples are presented in Fig. 6. Contrary to the case in RTA-annealed counterpart, no cracks are observed over the W54 sample. The I_{sc} values of all samples are observed to increase with P concentration. Similarly, V_{OC} values of the samples, except W54, are seen to increase, too. The examination of the R_s values of these samples reveals improvement with respect to RTA. A further investigation may involve comparison of the results by varying the annealing temperature and period in the tube furnace.

Table 3: The change of V_{oc} and I_{sc} values of the samples annealed at 650 °C for 60 s and 650 °C for 120 s in RTA under Ar flow with and without ARCs.

	Annealed @ 650 °C for 60 s				Annealed @ 650 °C for 120 s			
	Without ARCs		With ARCs		Without ARCs		With ARCs	
	I_{sc} (mA)	V_{oc} (mV)	I_{sc} (mA)	V_{oc} (mV)	I_{sc} (mA)	V_{oc} (mV)	I_{sc} (mA)	V_{oc} (mV)
W51	0.07	19.4	0.11	58.1	0.09	62.6	0.11	67.1
W52	0.57	51.0	0.77	80.2	0.41	75.9	0.87	91.5
W53	1.10	63.1	3.00	82.2	1.63	94.9	2.73	103.3
W54	1.40	86.7	1.03	90.2	0.14	51.6	0.36	54.2

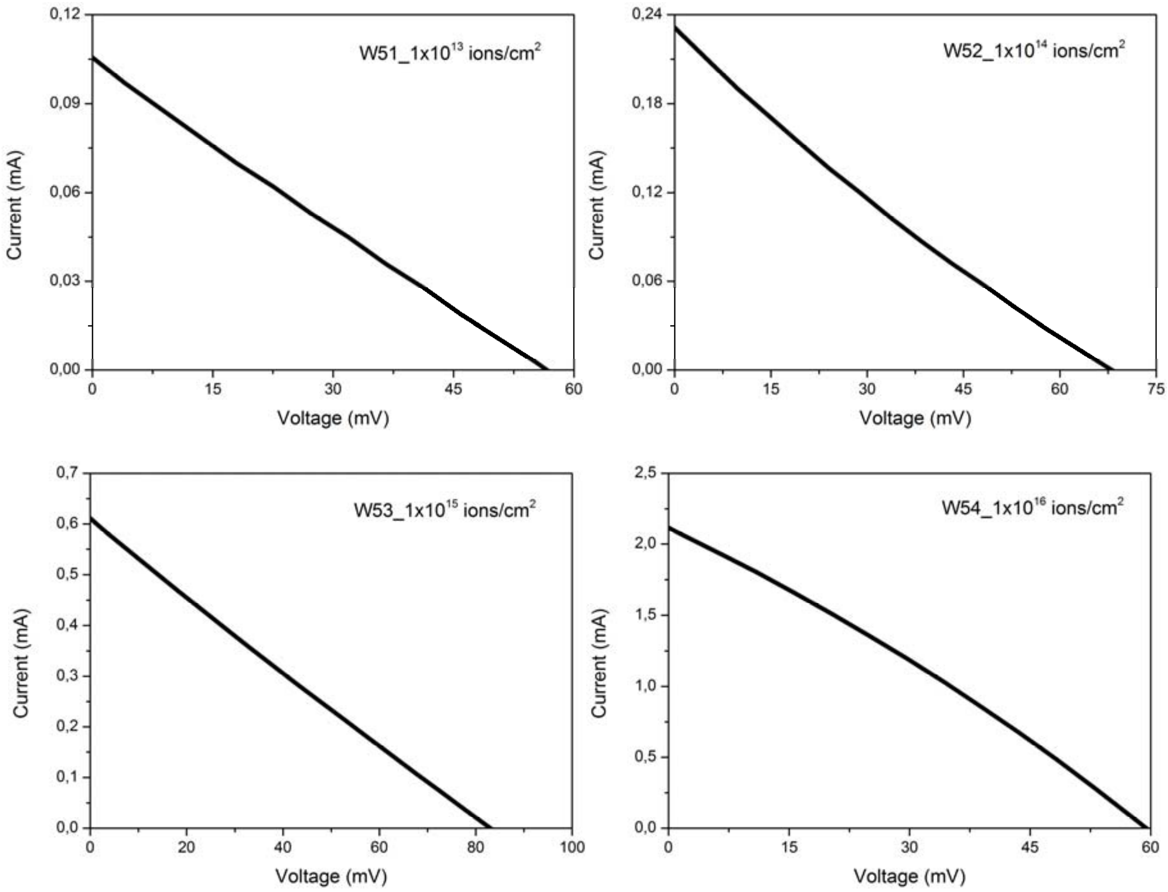

Fig. 6: The I-V measurement results of Ge samples implanted at different P concentrations after annealing at 700 °C for 30 minutes in a quartz tube furnace under N_2 environment.

4. Conclusıons

Ge solar cells are produced by ion implantation and their morphological and electrical properties with respect to the P dopant concentration are investigated. The I-V properties and the photovoltaic effects of the solar cells are investigated as a function of material and process parameters. An α-Si layer is introduced as an anti-reflection coating and good results are obtained. On the other hand, two different annealing procedures are applied to samples, where annealing in a tube furnace improves the outcome especially in the case of highly-doped samples.

Acknowledgements

The authors acknowledge the European Community (EC) as an Integrating Activity, “Support of Public and Industrial Research Using Ion Beam Technology (SPIRIT)”.

References

[1] B. De Jaeger, R. Bonzom, F. Leys, O. Richard, J. Van Steenbergen, G. Winderickx, E. Van Moorhem, G. Raskin, F. Letertre, T. Billon, M. Meuris, , M. Heyns, Microelectron. Eng., **80**, 26 (2005).

[2] C. Claeys, E. Simoen, Germanium – Based Technologies, Elsevier, The Boulevard, Langford Lane, Kidlington, Oxford, UK, (2007), pp. 23.

[3] J. Liu, J. Michel, W. Giziewicz, D. Pan, K. Wada, D.D. Cannon, S. Jongthammanurak, D.T. Danielson, L.C. Kimerling, , J. Chen, F.O. Ilday, F.X. Kartner, J. Yasaitis, Appl. Phys. Lett., **87(**10), 103501 (2005).

[4] N.E. Posthuma, J. Van der Heide, , G. Flamand, J. Poortmans, IEEE Trans. Electron Devices, **54**(5), 1210 (2007).

[5] J. Van der Heide, N.E. Posthuma, , G. Flamand, W. Geens, J. Poortmans, Sol. Energy Mater. Sol. Cells. **93**, 1810 (2009).

[6] A. Luque, S. Hegedus (Ed.), Handbook of Photovoltaic Science and Engineering, John Wiley & Sons, Chichhester, West Sussex, England, pp. 394, 2003.

[7] S. P. Tobin, S.M. Vernon, J. Bajgar, V.E. Haven, L.M. Geoffroy, D.R. Lillington, IEEE Electr. Dev. L. **9**, 256 (1988).

[8] S. J. Wojtczuk, S.P. Tobin, C.J. Keavney, C. Bajgar, M. M. Sanfacon, L. M. Geoffroy, T. M. Dixon, S. M. Vernon, J. D. Scofield, D. S. Ruby, IEEE T. Electron Dev., **37**, 455 (1990).

[9] N.H. Karam, R.R. King, B.T. Cavicchi, D.D. Krut, J.H. Ermer, M. Haddad, L. Cai, D.E. Joslin, M. Keyes, R.K. Ahrenkiel, IEEE T. Electron Dev. **46**, 2116 (1999).

[10] N.H Karam., R.R King., M. Haddad, J.H. Ermer, H. Yoon, H.L. Cotal, R. Sudharsanan, J.W. Eldredge, K. Edmondson, D.E Joslin., D.D. Krut, M. Takahashi, W. Nishikawa, M. Gillanders, J. Granata, P. Hebert, B.T. Cavicchi, D.R. Lillington, Sol. Energ. Mat. Sol. C., **66(**1), 453 (2001).

[11] D. Crisp, A. Pathare, R.C. Ewell, Acta Astronautica, **54**, 83 (2003).

[12] G. Timò, C. Flores, R. Campesato, Cryst. Res. Technol., **40**, 1043 (2005).

[13] M. Yamaguchi, T. Takamoto, K. Araki, N.E. Daukes, Sol. Energy, **79**, 78 (2005).

[14] M. Bosi, C. Pelosi, Prog. Photovolt. Res. Appl., **15**, 51 (2007).

[15] M. Yamaguchi, K.I. Nishimura, T. Sasaki, H. Suzuki, K. Arafune, N. Kojima, , Y. Ohsita, Y. Okada, A. Yamamoto, T. Takamoto, , K. Araki, Sol. Energy, **82**, 173 (2008).

[16] T. Markvart, L. Castañer (Ed.), Solar Cells: Materials, Manufacture and Operation, Elsevier, The Boulevard, Langford Lane, Kidlington, Oxford, UK, pp. 355, 2005.

[17] G. Sun, F. Chang, R.A. Soref, Optics Express **18**, 3746 (2010).

[18] C. Claeys, E. Simoen, Germanium - Based Technologies, Elsevier, The Boulevard, Langford Lane, Kidlington, Oxford, UK, pp. 233 (2007).

[19] P.D. Townsend, P.J. Chandler, , L. Zheng, Optical effects of ion implantation, Cambridge University Press, The Pitt Building, Trumpington Street, Cambridge, pp. 7 (1994).

[20] P.H. Holloway, G.E. McGuire, Handbook of Compound Semiconductors: Growth, Processing, Characterization and Devices, Noyes Publications, Mill Road, Park Ridge, New Jersey, USA, pp. 285. (1995).

---

[*] Corresponding author: ikabacelik@gmail.com